Theoretical Determination of Aqueous Acid-Base p*K* Values: Electronic Structure Calculations and Steered Molecular Dynamic Simulations

S. Tolosa,[a*] J.A. Sansón,[a] A. Hidalgo,[a] N. Mora-Diez[b*]

[a] Departamento de Ingeniería Química y Química Física, Universidad de Extremadura, Badajoz, Spain.

[b] Department of Chemistry, Thompson Rivers University, Kamloops, BC, V2C 0C8, Canada.

Abstract

The equilibrium constants (*K*) of several acid-base equilibria involving isomers of acetohydroxamic acid in aqueous solution are theoretically determined applying electronic structure methods (at the M06-2X-SMD/6-311++G(d,p) and MP2-PCM/6-311++G(d,p) levels of theory) and steered molecular dynamic (SMD) simulations. In the absence of experimental data and to validate the methods used, the aqueous acid-base process between formic acid and the acetate anion was also studied. Excellent agreement with experiment was obtained from SMD simulations that started from M06-2X-SMD optimized geometries. Of the four proton-transfer processes studied from the Z- and E-imide isomers to the OH-deprotonated Z-amide anion, the COH deprotonation of Z-imide is the most favorable process from a kinetic and thermodynamic points of view. Good qualitative agreement was found between the calculated p*K* values from electronic structure calculations and the SMD simulations. SMD simulations, when properly corrected, can be successfully used to evaluate Gibbs energy changes of acid-base reactions in solution and the corresponding p*K* values.

Keywords: aqueous p*K* calculations, acid-base equilibria, SMD simulations, M06-2X, MP2.

* Corresponding authors: santi@unex.es, nmora@tru.ca

1. Introduction

Thermodynamic studies, and in particular the determination of equilibrium constants (K, pK = - log K) in aqueous solution, are essential to properly understand a variety of systems of environmental and biochemical importance. Experimental challenges and the need for reliable physico-chemical data explain the growing interest in developing computational protocols for the accurate prediction of equilibrium constants [1-12].

Continuum solvation methods are the most practical way of accounting for solvent effects when calculating pK values in solution making use of electronic structure methods. Some studies have made use of a thermodynamic cycle that combines the equilibrium in the gas phase with the equivalent one in solution after calculating Gibbs energies of solvation of the species involved [13, 14]. Other studies apply solvation methods when optimizing and characterizing the geometries of the species involved and directly compute standard absolute Gibbs energies in solution [15, 16]. There have been numerous examples of pK calculations in which, in addition to the continuum, explicit solute-solvent interactions are accounted for by considering one or more explicit solvent molecules interacting with each of the species involved in a particular equilibrium system [17]. Qualitative structure-property relationships have also been successfully used to predict aqueous pK values [18].

This study focuses on the calculation of aqueous pK values of acid-base equilibria. When dealing with this type of system, the work with isodesmic reactions has led to more accurate pK determinations [16, 19]. Isodesmic reactions are hypothetical reactions in which the number of bonds of each formal type remains the same on each side of the equation but with changes occurring in their mutual relationships [20].

Classical molecular dynamic (MD) simulations are a desirable alternative approach for predicting the evolution of acid-base processes in time and to account for the molecular description of the solvent. The steered molecular dynamic (SMD) technique [21, 22], which applies external steering forces in a particular direction allow the calculation of Gibbs energy changes during the course of an elementary reaction.

Acetohydroxamic acid (AHA), also known as lithostat, is a drug used with antibiotics and/or surgery to treat certain types of bladder infections. AHA is also used as a chelating ligand for organometallic compounds. Other hydroxamic acids also have medical applications and play key roles as bioligands [23]. AHA is a complex system in aqueous solution. It can exist in four neutral forms, the amide and imide forms, in Z and E conformations each (see Figure 1). The Z-amide and E-amide forms are the most thermodynamically stable. The complete thermodynamic and kinetic study of the imide-amide tautomerisms in AHA was recently performed by our group applying both electronic structure methods (M06-2X-SMD/6-311++G(d,p) and MP2-PCM/6-311++G(d,p)) and SMD simulations [15].

Each neutral form of AHA has two acidic hydrogen atoms and can experience O- and N-deprotonation (the amide isomers: ZA and EA) or two different O-deprotonations (the imide isomers: ZI and EI) in aqueous solution. The eight possible dissociations produce five (with the MP2 method; see [24, 25]) or six (with the M06-2X method) different anionic forms shown in Figure 1, together with their relative Gibbs energies of formation at two levels of theory. These multiple dissociation equilibria contribute to the relatively low overall acid dissociation constants (K_a, pK_a = - log K_a) of this compound in aqueous solution. Several theoretical and experimental studies have dealt with the deprotonation and pK_a determination of AHA [24-27].

In this work, the aqueous equilibrium constant (K, pK = -log K) of four acid-base equilibria (shown in Figure 2) involving each of the imide isomers of AHA reacting with the O-deprotonated form of ZA, ZA(NO^-), to form an anionic form of the imide isomers and ZA molecule, are calculated applying electronic structure methods (at two levels of theory) and steered molecular dynamic (SMD) simulations. This is the first study in which SMD simulations are applied to determine aqueous pK values of acid-base equilibria.

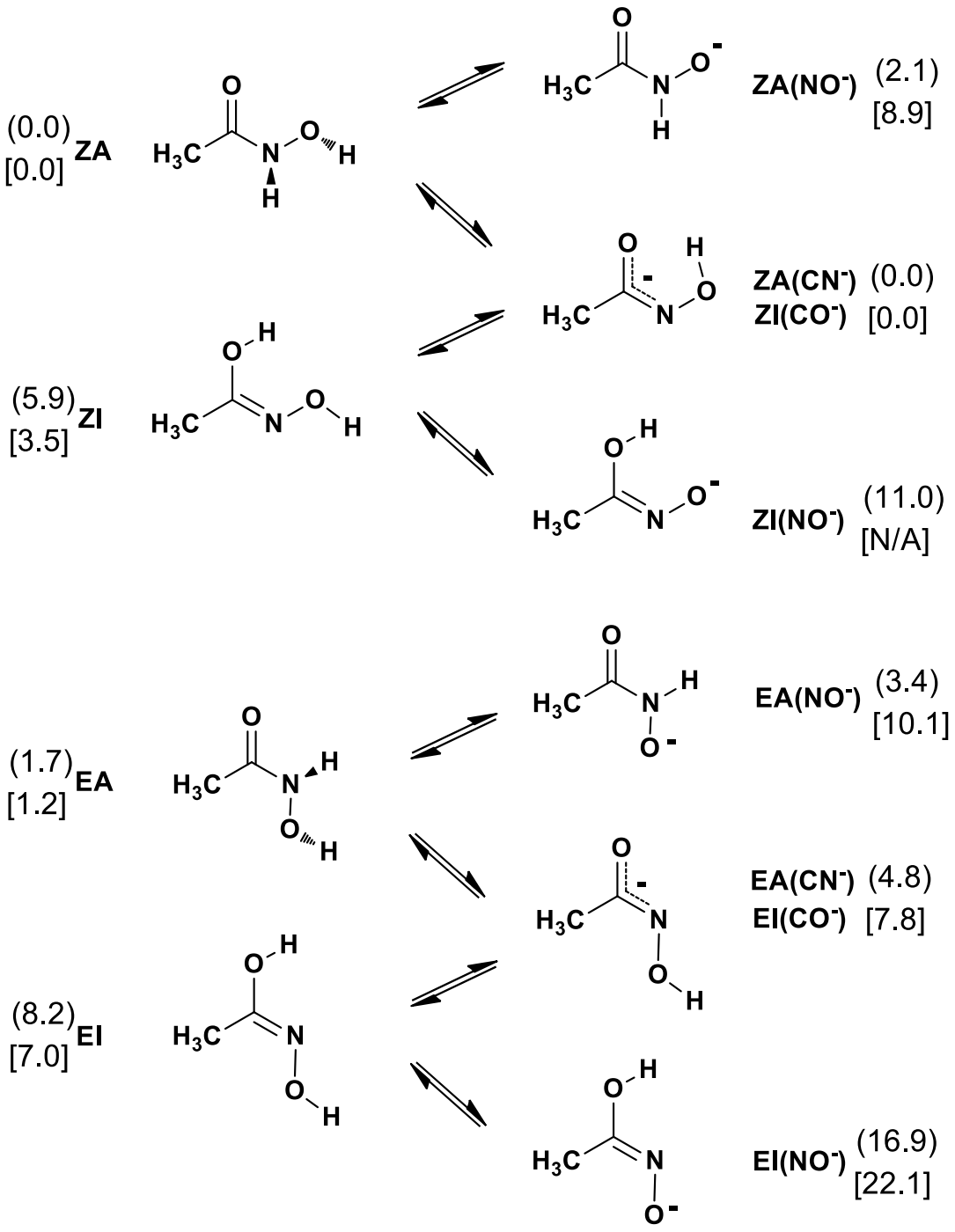

Figure 1. Most stable conformations of the AHA isomers and their possible dissociation products in aqueous solution calculated at the M06-2X-SMD/6-311++G(d,p) and MP2-PCM/6-311++G(d,p) levels of theory (relative Gibbs energies of formation are shown in parentheses and brackets for the M06-2X and the MP2 methods, respectively, at 298.15 K in kcal/mol).

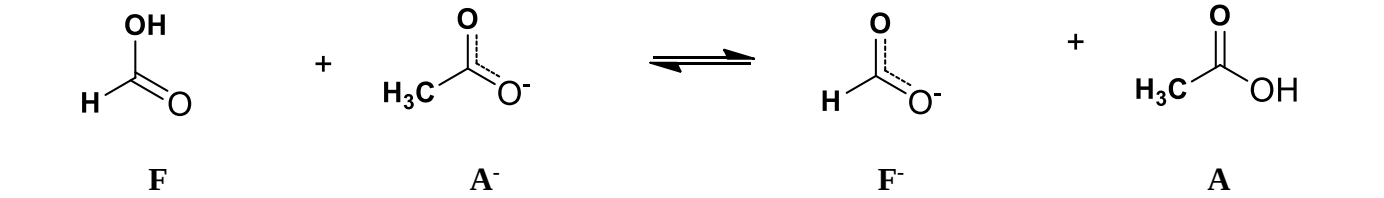

F **A$^-$** **F$^-$** **A**

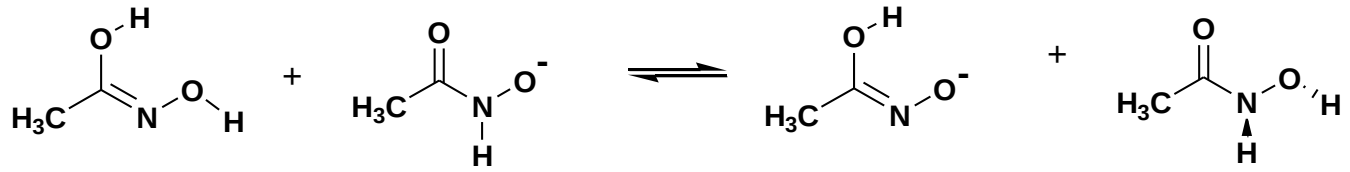

(a) **ZI** **ZA(NO$^-$)** **ZI(NO$^-$)** **ZA**

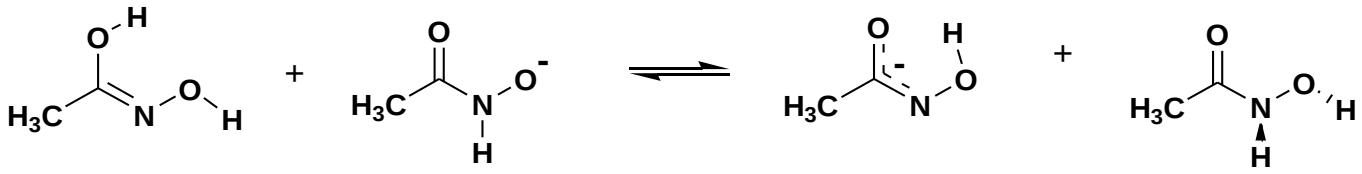

(b) **ZI** **ZA(NO$^-$)** **ZI(CO$^-$)** **ZA**

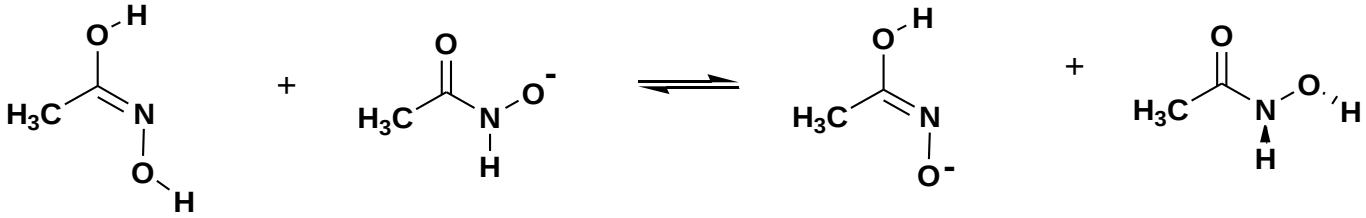

(c) **EI** **ZA(NO$^-$)** **EI(NO$^-$)** **ZA**

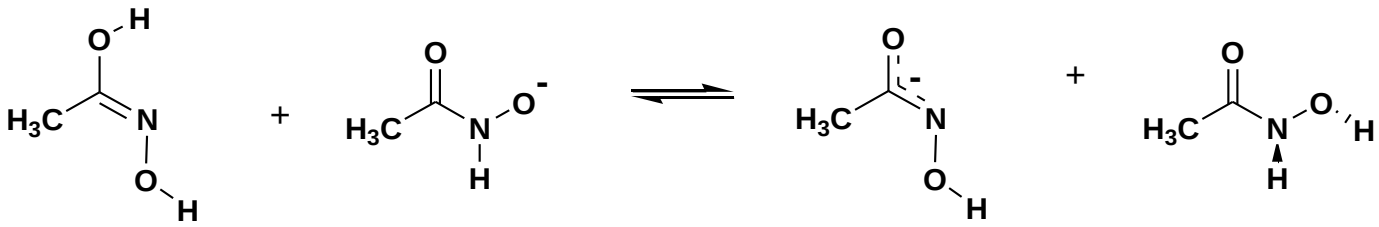

(d) **EI** **ZA(NO$^-$)** **EI(CO$^-$)** **ZA**

Figure 2. Acid-base equilibria studied.

2. Computational Details

2.1. Calculation of aqueous p*K* values

The calculation of p*K* values require the use of eq 1, where *R* is the ideal gas constant and *T* is the temperature in kelvin. The standard Gibbs energy change ($\Delta G°$) is calculated as the difference between the sum of the calculated standard absolute Gibbs energies ($G°$) of the products and of the reactants (stoichiometric coefficients are assumed to be 1), as if using their corresponding standard Gibbs energies of formation ($\Delta_f G°$) using eq 2.

$$\mathrm{p}K = \frac{\Delta G^{\circ}}{RT\log 10} \tag{1}$$

$$\Delta G° = \Sigma \Delta_f G° \text{ (products)} - \Sigma \Delta_f G° \text{ (reactants)} \tag{2}$$

For the acid ionization reaction shown in Scheme 1, the aqueous thermodynamic pK_a of the acid HA is the experimental value of the equilibrium quotient extrapolated at ionic strength zero.

$$HA_{(aq)} \leftrightarrows A^-_{(aq)} + H^+_{(aq)} \qquad \text{Scheme 1}$$

As previously introduced, theoretical determinations of aqueous pK_a values are more accurate when performed relative to another acid (HB) of similar chemical structure, as shown in Scheme 2.

$$HA_{(aq)} + B^-_{(aq)} \leftrightarrows A^-_{(aq)} + HB_{(aq)} \qquad \text{Scheme 2}$$

In such cases, the aqueous thermodynamic pK_a of HA is calculated using eq 3, in which the experimental aqueous pK_a of the reference acid is needed, p$K_{a\,(HB)}$, and $\Delta G°$ in solution is calculated according to eq 4.

$$pK_{a\ (\mathrm{HA})} = \frac{\Delta G^{o}}{RT\log 10} + pK_{a\ (\mathrm{HB})} \tag{3}$$

$$\Delta G^{\circ} = \Delta_f G^{\circ}_{(\mathrm{A}^-)} + \Delta_f G^{\circ}_{(\mathrm{HB})} - \Delta_f G^{\circ}_{(\mathrm{HA})} - \Delta_f G^{\circ}_{(\mathrm{B}^-)} \tag{4}$$

The acid-base equilibria shown in Figure 2 are of the type described in Scheme 2. The two O-deprotonations from Z-imide (ZI) and E-imide (EI), relative to the O-deprotonation of the most thermodynamically stable acid form, Z-amide (ZA), are studied. Eqs 3 and 4 become Eqs 5 and 6 when applied to the ZI→ZI(NO^-) equilibrium depicted in Figure 2.

$$pK_{a\ (ZI\rightarrow ZI(NO^-))} = \frac{\Delta G^{o}}{RT\log 10} + pK_{a\ (ZA\rightarrow ZA(NO^-))} \tag{5}$$

$$\Delta G^{\circ} = \Delta_f G^{\circ}_{(\mathrm{ZI(NO^-)})} + \Delta_f G^{\circ}_{(\mathrm{ZA})} - \Delta_f G^{\circ}_{(\mathrm{ZI})} - \Delta_f G^{\circ}_{(\mathrm{ZA(NO^-)})} \tag{6}$$

Given the complexity of AHA in aqueous solution and the fact that its experimental pK_a value, reported to be in the 9.02–9.40 range [24, 28, 29], is not solely determined by a single acid dissociation and that an experimental value for the thermodynamic pK_a of the ZA isomer dissociating to form the ZA(NO^-) anion is not available, we are unable to rigorously apply eq 5 to determine the site specific pK_a values of the neutral isomers depicted in Figure 2. However, we can apply eqs 6 and 1 to determine the aqueous pK of these acid-base equilibria. The purpose of this paper is to perform this task with electronic structure methods and SMD simulations to compare the performance of these two distinctive theoretical approaches. To validate the methods used, the additional acid-base equilibrium between formic acid and acetate (shown in Figure 2), for which an experimental value exists, was also studied.

2.2. Electronic structure calculations

Calculations have been performed using the GAUSSIAN 09 software package [30]. Geometries have been fully optimized and characterized at the MP2/6-311++G(d,p) level of theory. Solvent effects are accounted for on the geometry optimizations and frequency calculations by means of

the IEF-PCM [31] method, employing the UFF atomic radii when constructing the solvent cavity. Mulliken charges [32] in solution were used to calculate the initial intermolecular potential used in the MD simulations and to perform an initial acidity comparison of the four cases studied. Additional calculations have been performed using the M06-2X [33] functional and the 6-311++G(d,p) basis set in combination with the SMD solvation method [34] on both geometry optimizations and frequency calculations.

2.3. MD simulations

To describe the solute-solvent interaction potential, a LJ (12-6-1) function was used

$$U_{sw} = \sum_{ij} \frac{A_{ij}^{sw}}{r_{ij}^{12}} - \sum_{ij} \frac{B_{ij}^{sw}}{r_{ij}^{6}} + \sum_{ij} \frac{q_i^s q_j^w}{r_{ij}} \tag{7}$$

where the A_{ij} and B_{ij} van der Waals parameters were taken from the AMBER force field [35] for each type of atom instead of from quantum calculations, because of the great computational effort involved. This choice takes into account that the van der Waals component is only a small fraction of the total interaction energy. However, due to the importance of the electrostatic component in this type of studies the net charges on each solute atom q_i^s, used in eq. 7, are initially obtained with the Mulliken procedure [32], whereas the charges of the solvent atoms q_j^w are pre-assigned as the TIP3P charges [36], i.e., δ(O) = -0.83 and δ(H) = 0.415.

The potential of mean force (PMF) in a reaction represents the free energy change with the reaction coordinate. To relate Gibbs energy differences between two equilibrium states and non-equilibrium processes, the Jarzynski's equality [37] is used. So, this free energy change, Δ*G*, is related to an average over all possible works <*W*> of an external process that take the system from the equilibrium state A to a new state B, as shown by eq. 8:

$$\Delta G = \langle W \rangle - \frac{1}{2K_B T} \left(\langle W^2 \rangle - \langle W \rangle^2 \right), \tag{8}$$

where *W* is calculated by integrating the force over the distance of the steered atom from its initial to final position, according to eq. 9.

$$W = -\int_0^t F \cdot dr = \frac{1}{2} k \int \left(vt - (r_{(t)} - r_{(o)})^2 \right) dr \, . \tag{9}$$

The MD simulations with periodic boundary conditions for each system in an aqueous environment, formed by about 200 water molecules depending on the system considered, were carried out at 298.15 K using the AMBER program [38]. Water molecules initially located at distances less than 1.6 Å from any solute atom were eliminated from the simulations. The long-range electrostatic interactions were treated by the Ewald method [39]. A cut-off of 7 Å was applied to the water–water interactions in order to simplify the calculations, and periodic boundary conditions were used to keep the number of solvent molecules constant.

In order to perform the SMD simulations, the QM/MM method with the semi-empirical QM Hamiltonian SCC-DFTB [40, 41], implemented in the AMBER12 software [42, 43] was used. The system was initially minimized with a 1 ps simulation. Subsequently, the system was equilibrated at 100 ps in order to obtain an initial configuration to begin the phase propagation and data storage. Finally, during the last 100 ps of the simulation the position and velocity of each atom were stored and all the atoms of AHA (except the hydrogen ion being transferred) were kept fixed. The force constant used was 1000 kcal/mol·Å^2 for the distance, and the hydrogen ion being transferred was directed from the imide to the amide anion structure. The reaction coordinates chosen for describing the proton transfer processes are discussed in the next section.

SMD simulations allow the calculation of Gibbs energy profiles. Hence, the standard Gibbs energies of activation ($\Delta^{\neq}G^o$) and reaction (ΔG^o) can be determined following the time-evolution of the process, i.e., from the configuration of the reactant to the product configuration in an elementary step focusing on the reaction coordinate. The stationary points involved in the reaction mechanism can be visualized to represent the evolution of the system every step of the process.

Calculated ΔG^o values from SMD simulations need to be corrected to be properly compared with values calculated applying electronic structure methods. This correction arises from the fact that, due to computational practical considerations, the simulation does not start at an infinite separation between the interacting species. Corrected ΔG values are obtained by subtracting the sum of the $\Delta_f G°$ of the isolated reactants (and products). To this end, quantum calculations of reactant (and product) systems at their isolated configurations were also performed. The energy differences between the reactants (and products) with the simulation structure with respect to the isolated molecules lead to a correction of $\Delta G°$ energy that will be hereinafter denoted as SMD-corrected (ΔG), and it is represented in Scheme 3.

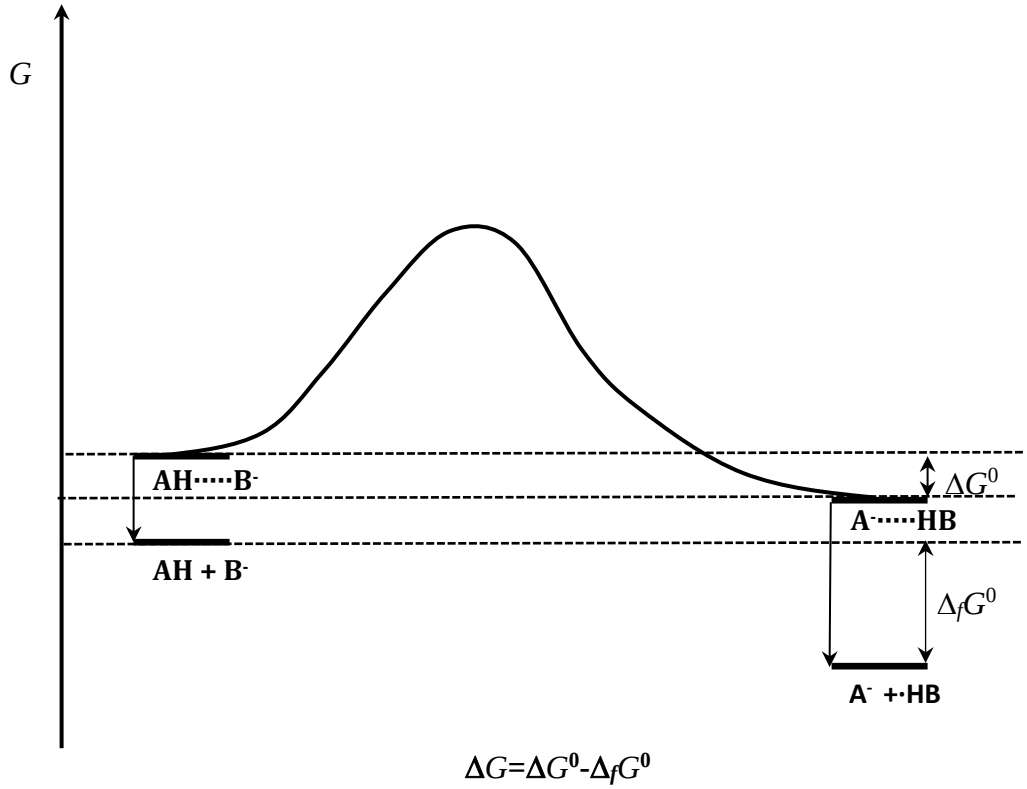

Scheme 3. Graphical representation of the method to calculate the SMD-corrected energy

3. Results and Discussion

3.1. Equilibria studied

Initially, a brief study of acid-base equilibrium between carboxylic acids (Formic acid (F) + Acetate anion (A^-) ⇆ Formate anion (F^-) + Acetic acid (A)) was performed as reference test taking into account the availability of p*K* experimental values of these acids and the simplicity of the deprotonation process given that only one type of proton transfer is possible (see the top equilibrium of Figure 2). Afterwards, several Imide + ZA(NO^-) ⇆ Imide-anion + ZA equilibria were also studied applying electronic structure methods, in which solvent is treated as a continuum, and through SMD simulations, in which the solvent is treated as a discrete medium. The four acid-base AHA processes considered and the acronyms used to identify the species involved are shown in Figure 2 (a to d). In these processes, the hydrogen atom on the -NOH (oxime) or on the -COH (enol) groups of the ZI and EI isomers is transferred to the NO^- group of the ZA(NO^-) anion to form the ZA neutral acid and the corresponding ZI^- and EI^- imide anions.

The reaction coordinate considered to carry out the SMD simulations in these processes was the distance RC = $d(O_S\text{-}H_S)$ -$d(H_S\text{-}O_{ZA}^-)$, where *S* and *ZA* represent the atoms of the isomer (S = ZI, EI) involved in the proton transfer. The initial orientation and separation between the reactant molecules was set to an $O_S\cdots O_{ZA}$ distance of 3 Å and the ($O_S\text{-}H\cdots O_{ZA}$) bond angle was set to 180º. Cartesian coordinates of each of the optimized species are reported in the Supporting Information.

3.2. Reaction free energies from quantum calculations

Reaction free energies of all processes studied by electronic structure calculations are presented in Table 1. The standard absolute enthalpies and Gibbs energies, as well as the Cartesian coordinates of each species considered in this study are shown in Tables S1 and S3, respectively, of the Supporting Information. As previously reported [24], the ZI(NO^-) anion cannot be optimized at the MP2-PCM level of theory, which explains the lack of a calculated value for equilibrium (a) at this level of theory.

Table 1. Standard aqueous Gibbs energy of reaction (ΔG^o, in kcal/mol at 298.15 K) calculated from electronic structure methods (M06-2X-SMD and MP2-PCM) and from SMD simulations.

Acid-Base Equilibria	M06-2X-SMD[a]	MP2-PCM[a]	SMD[b]	SMD-corrected[a]
$F + A^- \leftrightarrows F^- + A$[e]	-4.3	-5.9	-3.2[c] (-5.3)[d]	-1.3[c] (-3.2)[d]
(a) $ZI + ZA(NO^-) \leftrightarrows ZI(NO^-) + ZA$	3.1	-	2.8 (4.0)	4.4 (5.7)
(b) $ZI + ZA(NO^-) \leftrightarrows ZI(CO^-) + ZA$	-7.9	-12.4	-13.1 (-3.5)	-11.6 (-3.6)
(c) $EI + ZA(NO^-) \leftrightarrows EI(NO^-) + ZA$	6.7	6.2	5.9 (3.7)	8.7 (10.9)
(d) $EI + ZA(NO^-) \leftrightarrows EI(CO^-) + ZA$	-5.5	-8.1	-7.5 (-3.7)	-3.4 (-0.3)

[a] Calculated as: $\Delta G° = \Delta_f G°(F^-, ZI^- \text{ or } EI^-) + \Delta_f G°(A \text{ or } ZA) - \Delta_f G°(F, ZI \text{ or } EI) - \Delta_f G°(A^- \text{ or } ZA(NO^-)$.
[b] Obtained from PMF in SMD simulation.
[c] Using M06-2X-SMD initial geometries.
[d] Using MP2-PCM initial geometries.
[e] The experimental ΔG^o is -1.36 kcal/mol.

Both combinations of electronic structure calculations are able to reproduce the negative sign of the experimental ΔG^o (-1.36 kcal/mol) of the equilibrium involving the carboxylic acids, with more than 2.5 kcal/mol units of error. The error of the MP2-PCM calculation is larger than that of the M06-2X-SMD calculation.

The calculated sign for the ΔG^o involving AHA species is equally determined by both methods, but the MP2-PCM results are consistently smaller than the M06-2X-SMD values. The largest difference between these two sets of calculations is 4.5 kcal/mol. The two COH deprotonations are exergonic while the NOH ones are endergonic, which agrees with previous studies by Senent et al. [24, 25] and Dissanayake et al. [26].

3.3. Reaction free energies from SMD simulations

As previously explained in section 2.3., the reaction free energies from SMD simulations need to be corrected so that the calculated quantities can be properly compared to those obtained from electronic structure calculations. This correction is so that the initial and final state in both types

of calculations is the same, because the SMD simulation starts from a point in which both reactant species are separated 3 Å. However, when the calculation is done using electronic structure methods, the reactant and product species are infinitely separated. The Gibbs energies of reactants and products used to determine this correction are reported in Table S2 of the Supporting Information. The reaction free energy values from SMD simulations (with and without correction) are reported in Table 1 and the energy profiles are displayed in Figure 3.

When focusing on the formic acid-acetate equilibrium, the SMD values that use M06-2X-SMD initial geometries lead to ΔG^{o} values that are closer to experiment than the values calculated with electronic structure methods, and the corrected value of -1.25 kcal/mol is the one in closest agreement with experiment (with an error of 0.11 kcal/mol).

In general, the SMD simulation results agree qualitatively with those obtained applying electronic structure methods. The two COH deprotonations are exergonic while the NOH ones are endergonic. In addition, the corrected SMD values (starting from M06-2X-SMD geometries) are in closer agreement with the M06-2X-SMD values with differences from 1.3 (equilibrium (a)) to 3.7 (equilibrium (b)) kcal/mol.

Figure 3 shows the evolution of free energy when the proton is transferred during the simulation. From the energy curves of the deprotonation reactions of the ZI and EI isomers, one can say that there is a change in the spontaneity of the process depending on which is the donor group, namely, the process is exergonic when deprotonation occurs from the enolic oxygen and endergonic when it occurs from the oximic oxygen. Furthermore, the deprotonation from EI(NOH) using M06-2X-SMD geometry presents a high barrier (of about 48 kcal/mol), which is significantly reduced in the EI(COH) deprotonation ($\Delta G^{\ddagger}_{M06}$(COH) = 35 kcal/mol) and also when the MP2-PCM initial geometry is used ($\Delta G^{\ddagger}_{MP2}$(NOH) = 37 kcal/mol). According to this, the ZI(COH) deprotonation process is the most favorable due to its higher speed and spontaneity for all cases considered.

Analyzing the configurations at each step of the simulation we can find the structures in the activation region and for the reaction products (the Cartesian coordinates for transition states and

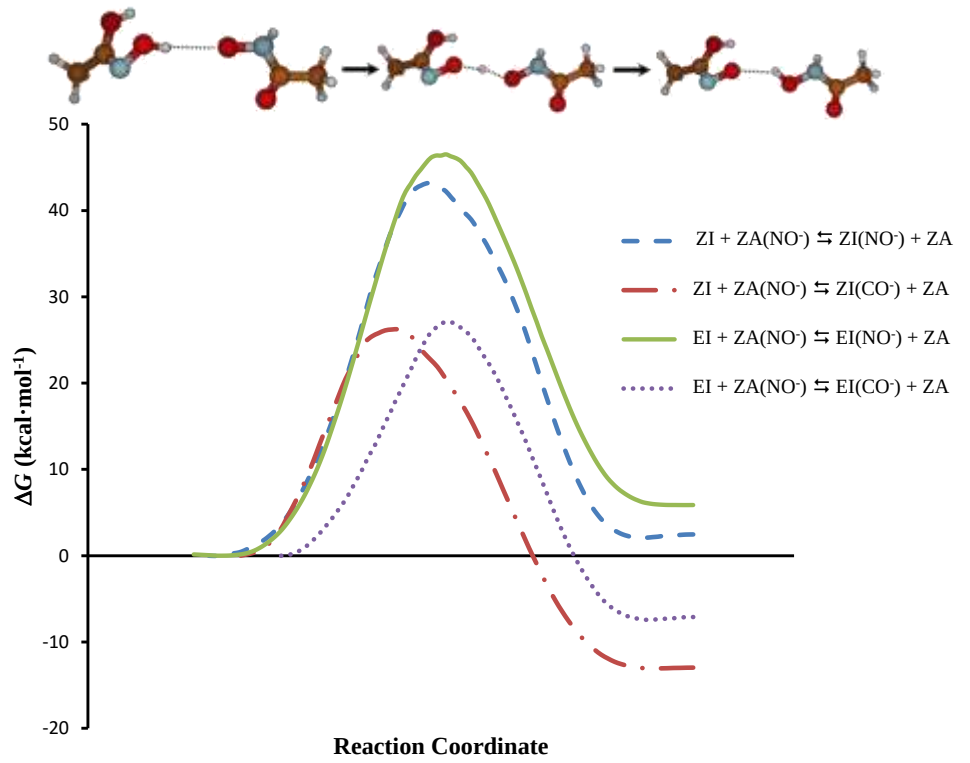

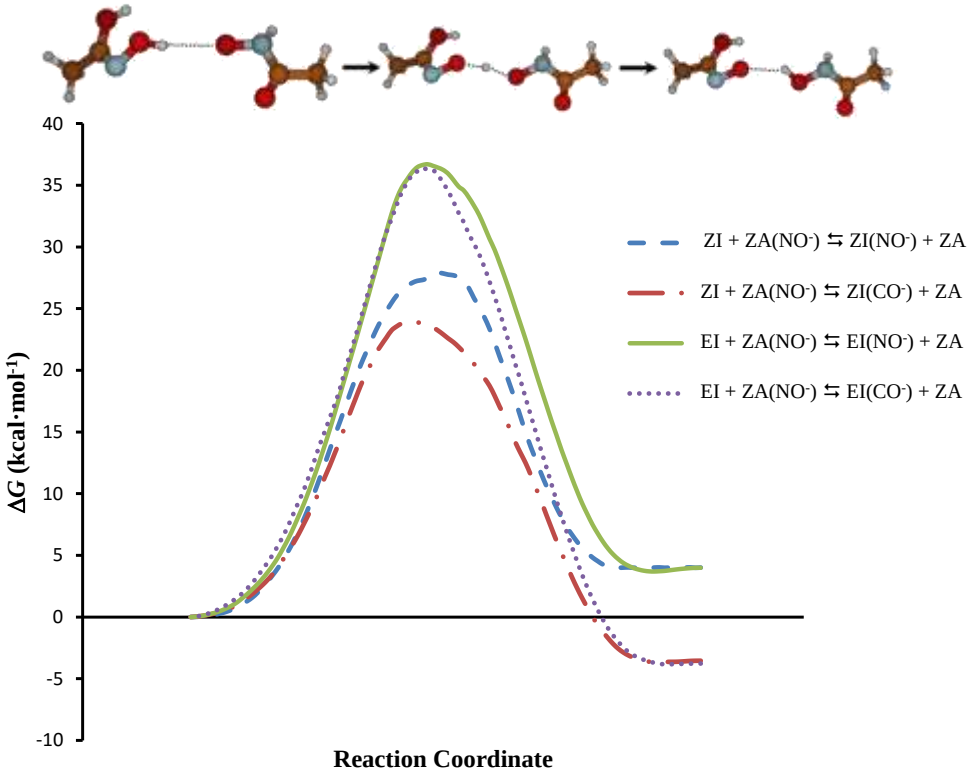

Figure 3. PMF for the deprotonation processes of the ZI and EI isomers using M06-2X-SMD (top) and MP2-PCM (bottom) geometries.

product structures are reported in Table S4 of the Supporting Information). Considering as an example the (a)-process with MP2-PCM initial geometries, schematically depicted at the top of Figure 3, the reactants (in its initial configuration $d_{O(ZI)-H(ZI)}$ = 1 Å, $d_{H(ZI)\cdots O(ZA)}$ = 2.12 Å, and θ_{OHO}=180º) evolve to a higher energy state where the transferred proton is located at 1.55 Å away from the oxygen atom acting as donor and at 1.58 Å from the acceptor oxygen atom, forming a bond angle of 168º. In the final step the proton is found at $d_{O(ZI)\cdots H(ZI)}$ = 2.38 Å, $d_{H(ZI)-O(ZA)}$ = 0.96 Å, and θ_{OHO}=160º. Similar comments can be made for the rest of the processes considered in this work.

3.4. p*K* calculations

As previously discussed, the experimental data (ΔG^o and p*K* values) for the formic acid-acetate equilibrium is best reproduced by the corrected-SMD simulations starting from M06-2X-SMD geometries. The p*K* value is calculated with an error of 0.08 units.

The calculated p*K* values of the different acid-base processes considered are reported in Table 2, relative to the Z-amide dissociation to the ZA(NO^-) anion. Therefore, a negative value of p*K* (that results from a negative ΔG^o value, see eq 1) indicates that a particular deprotonation of the imide isomer is more favorable than that of the Z-amide form (into the ZA(NO^-) anion). Hence, such a species is a stronger acid that ZA_{NOH}.

Analyzing the p*K* values obtained for the AHA equilibria from electronic structure calculations and SMD simulations, the same acid-base strength sequence can be qualitatively (except when the SMD simulations use initial MP2-PCM geometries), which is consistent with other studies [25, 26]:

$$pK\ (c, EI_{NOH}) > pK\ (a, ZI_{NOH}) > pK\ (d, EI_{COH}) > pK\ (b, ZI_{COH})$$

In agreement with the predictions of Dissanayake [26], the NOH deprotonation leads to larger p*K* values that the COH deprotonations from each of the imide isomers. Each of the E-imide

deprotonations are less favourable than the corresponding Z-imide deprotonations, relative to the Z-amide deprotonation (ZA_{NOH}).

Table 2. Calculated p*K* values in aqueous solution at 298.15 K using eq 1 and the ΔG^o values displayed in Table 1.

Acid-Base Equilibria	M06-2X-SMD	MP2-PCM	SMD	SMD-corrected	Others
$F + A^- \leftrightarrows F^- + A$	-3.12	-4.33	2.45[a] (0.92)[b]	-0.92[a] (-2.33)[b]	-1.0[c]
(a) $ZI + ZA(NO^-) \leftrightarrows ZI(NO^-) + ZA$	2.27	-	2.05 (2.93)	3.20 (4.18)	-
(b) $ZI + ZA(NO^-) \leftrightarrows ZI(CO^-) + ZA$	-5.79	-9.09	-9.57 (-2.57)	-8.47 (-2.64)	-
(c) $EI + ZA(NO^-) \leftrightarrows EI(NO^-) + ZA$	4.89	4.54	4.31 (2.71)	6.34 (8.00)	-
(d) $EI + ZA(NO^-) \leftrightarrows EI(CO^-) + ZA$	-4.03	-5.94	-5.50 (-2.71)	-2.52 (-0.22)	-

[a] Values using $\Delta G_{M06\text{-}2X\text{-}SMD}$ from SMD simulations.
[b] Values using $\Delta G_{MP2\text{-}PCM}$ from SMD simulations.
[c] Experimental p*K* obtained using the experimental pK_a values of acetic acid (4.75) and formic acid (3.75).

4. Conclusions

The aqueous p*K* values of several acid-base equilibria involving isomers of acetohydroxamic acid have been calculated applying electronic structure methods (at the M06-2X-SMD/6-311++G(d,p) and MP2-PCM/6-311++G(d,p) levels of theory) and SMD simulations. Of the four proton-transfer processes studied from the Z- and E-imide isomers to the NOH-deprotonated Z-amide species, the COH deprotonation of Z-imide is the most favorable process from a kinetic and thermodynamic points of view. Good qualitative agreement was found between the calculated p*K* values from electronic structure calculations and the SMD simulations. SMD simulations, when properly corrected, can be successfully used to evaluate Gibbs energy changes of acid-base reactions in solution and the corresponding p*K* values.

Given the results obtained for the formic acid-acetate equilibrium, the corrected SMD results that start from M06-2X-SMD geometries seem to lead to the best results reported in this paper. Given the consistent closer agreement between these SMD simulations and the M06-2X-SMD results, these would be the most trusted electronic structure calculations presented in this paper. However, more simulations on acid-base systems from which there are reliable experimental data would be desirable.

Supporting Information

Tables S1 and S2 display the calculated thermodynamic data. Table S3 contains the M06-2X-SMD/6-311++G(d,p) and MP2-PCM/6-311++G(d,p) Cartesian coordinates of each calculated reactant and product species. Table S4 shows the Cartesian coordinates obtained from SMD simulations.

Acknowledgements

This research was sponsored by the Consejería de Infraestructuras y Desarrollo Tecnológico de la Junta de Extremadura (Project GR15003) and the Natural Sciences and Engineering Research Council of Canada (NSERC).

References

(1) Warshel A (1991) Computer Modeling of Chemical Reactions in Enzymes and Solutions. Wiley & Sons, New York

(2) Muller A, Ratjczak H, Junge W (1992) Electron and Proton Transfer in Chemistry and Biology. Elsevier, Amsterdam

(3) Cramer CJ, Truhlar DG (1994) Structure and Reactivity in Aqueous Solution: Characterization of Chemical and Biological Systems. American Chemical Society, Washington D.C.

(4) Bala P, Grocowski P, Lesyg B, McCammon JA (1995) Quantum Mechanical Simulation Methods for Studying Biological Systems. Springer, Berlin

(5) Aqvist J (1997) Modelling of Proton Transfer Reactions in Enzymes. In: Naray-Szabó G, Warshel A (eds) Computational Approaches to Biochemical Reactivity. Kluwer Academic Publisher, Netherlands, pp 341-362

(6) Náray-Szabó G, Warshel A (2002) Computational Approaches to Biochemical Reactivity. Springer, Berlin

(7) Tapia O, Bertrán J (2003) Solvent Effects and Chemical Reactivity. Springer, Berlin

(8) Binder K, Ciccotti G, Ferrario M (2006) Computer Simulations in Condensed Matter Systems: From Materials to Chemical Biology Vol. 2. Springer, Berlin

(9) Kotz JC, Treichel PM, Townsend J (2009) Chemistry and chemical reactivity. Thomson Higher Education, Belmont

(10) (a) *Ho J, Coote ML, Theor. Che. Acc.* ***2010****, 125, 3-21. (b)* Ho J, Klamt A, Coote ML (2010) *J Phys ChemA* **2010**, *114*, 13442-13444

(11) Stumm W, Morgan JJ, *Aquatic Chemistry: Chemical Equilibria and Rates in Natural Waters*, Wiley-Interscience: New York, 1996

(12) Thomas G, *Medicinal Chemistry: An Introduction*; John Wiley & Sons: West Sussex, 2000

(13) Shields GC, Seybold PG, "Computational Approaches for the Prediction of pK_a values", CRC Press, Taylor & Francis Group, Boca Raton, N.Y., 2014

(14) Casasnovas R, Ortega-Castro J, Frau J, Donoso J, Muñoz F, *Int. J.Quant.Chem.* **2014**, *114*, 1350–1363

(15) Tolosa S, Mora-Diez N, Hidalgo A, Sansón J, *RSC Adv.* **2014**, *4*, 44757-44768

(16) Brown TN, Mora-Diez N, *J. Phys. Chem. B* **2006**, *110*, 9270-9279

(17) See for example: (a) **Pliego JR, Riveros JM,** *J. Phys. Chem. A* **2002**, 106, 7434–7439; (b) Bryantsev VS, Diallo MS, Goddard WA, *J. Phys. Chem. B* **2008**, *112*, 9709-9719

(18) See for example: (a) Karelson M, Lobanov VS, Katritzky AR, *Chem. Rev.* **1996**, *96*, 1027-1044. (b) Hennemann M, Clark T, *J. Mol. Model.* **2002**, *8*, 95-101. (c) Soriano E, Cerdán S, Ballesteros P, *J. Mol. Struct. (THEOCHEM)* **2004**, *684*, 121-128. (d) Brown TN, Mora-Diez N, *J. Phys. Chem. B* **2006**, *110*, 20546-20554

(19) See for example: (a) Poliak P, *Acta Chimica Slovaca* **2014**, *7*, 25-30. (b) Sastre S, Casasnovas

R, Muñoz F, Frau J, *Theor. Chem. Acc.* **2013**, *132*, 1310. (c) Biswas AK, Lo R, Ganguly B, *Synlett*, **2013**, *24*, 2519–2524. (d) Derbel N, Clarot I, Mourer M, Regnouf-de-Vains J, Ruiz-Lopez MF, *J. Phys. Chem. A* **2012**, *116*, 9404–9411. (e) Govender KK, Cukrowski I, *J Phys ChemA* **2010**, *114*, 1868–1878. (f) Govender KK, Cukrowski I, *J Phys Chem A* **2009**, *113*, 3639–3647. (g) Li GS, Ruiz-Lopez MF, Maigret B, *J Phys Chem A* **1997**, *101*, 7885– 7892

(20) (a) Hehre WJ, Ditchfield R, Radom L, Pople JA, *J. Am. Chem. Soc.* **1970**, *92*, 4796–4801. (b) Ponomarev DA, Takhistov VV, *J. Chem. Ed.* **1997**, *74*, 201-203

(21) Izrailev S, Stepaniants S, Isralewitz B, Kosztin D, Lu H, Molnar F, Wriggers W, Schulten K,*Steered Molecular Dynamics. In: Computational Molecular Dynamics, Challenges, Methods, Ideas, Vol. 4 of Lectures Notes in Computational Science and Engineering*, Deuflhard P, Hermans J, Leimkuhler B, Mark AE, Reich S, Skell RD (eds), 1998, Springer-Verlag, Berlin, pp 39-65

(22) Isralewitz B, Gao M, Schulten K, *Curr.Opin.Struct. Biol.* **2001**, *11*, 224-230

(23) (a) Kakkar R, *Hydroxamic Acids: A Unique Family of Chemicals with Multiple Biological Activities*, Ed: S.P- Gupta, Sprìnger, 2013. *(b) Brown DA, Chidambaram MV, Metal Ions in Biological Systems; Marcel Dekker: New York, 1982; Vol. 14*

(24) Senent ML, Niño A, Muñoz Caro C, Ibeas S, García B, Leal JM, Secco F, Venturini M, *J. Org. Chem.* **2003**, *68*, 6535-6542

(25) Mora-Diez N, Senent ML, García B, *Chem. Phys.* **2006**, *324*, 350-358

(26) Dissanayake DP, Sentilnithy R, *J. Mol. Struct. (THEOCHEM)* **2009**, *910*, 93-98

(27) Bagno A, Comuzzi C, Scorrano G, *J. Am. Chem. Soc.* **1999**, *116*, 916-924

(28) (a) Monzyk B, Crumbliss AL, *J. Org. Chem.* **1980**, *45*, 4670-4675. (b) Brink CP, Fish LL, Crumbliss AL, *J. Org. Chem.* **1985**, *50*, 2277-2281

(29) Wise WM, Brandt WW, *J. Am. Chem. Soc.* **1955**, 77, 1058-1059

(30) Frisch MJ, Trucks GW, Schlegel HB, Scuseria GE, Robb MA, Cheeseman JR, Scalmani G, Barone V, Mennucci B, Petersson GA, Nakatsuji H, Caricato M, Li X, Hratchian HP, Izmaylov AF, Bloino J, Zheng G, Sonnenberg JL, Hada M, Ehara M, Toyota K, Fukuda R, Hasegawa J, Ishida M, Nakajima T, Honda Y, Kitao O, Nakai H, Vreven T, Montgomery JA Jr, Peralta JE, Ogliaro F, Bearpark M, Heyd JJ, Brothers E, Kudin KN, Staroverov VN, Kobayashi R, Normand J, Raghavachari K, Rendell A, Burant JC, Iyengar SS, Tomasi J, Cossi M, Rega N, Millam JM, Klene M, Knox JE, Cross JB, Bakken V, Adamo C, Jaramillo J, Gomperts R, Stratmann RE, Yazyev O, Austin AJ, Cammi R, Pomelli C, Ochterski JW, Martin RL, Morokuma K, Zakrzewski VG, Voth GA, Salvador P, Dannenberg JJ, Dapprich S, Daniels AD, Farkas Ö, Foresman JB, Ortiz JV, Cioslowski J, Fox DJ (2009) Gaussian 09, Revision A.1. Gaussian, Wallingford, CT

(31) MiertušS, Tomasi J, *Chem. Phys.* **1982**, *65*, 239-245. (b) Scalmani G, Frisch MJ, *J. Chem. Phys.* **2010**, *132*, 114110

(32) Mulliken RS, *J. Chem. Phys.* **1955**, *23*, 1833-1840

(33) Zhao Y, Truhlar DG, *Theor. Chem. Acc.* **2008**, *120*, 215-241

(34) (a) Marenich AV, Cramer CJ, Truhlar DG, *J. Phys. Chem. B* **2009**, *113*, 6378-xxx. (b) Cramer CJ, Truhlar DG, *SMx Continuum Models for Condensed Phases" in Trends and Perspectives in Modern Computational Science*; Lecture Series on Computer and Computational Sciences Vol. 6; Maroulis, G., Simos, T. E., Eds.; Brill/VSP, Leiden, 2006; pp. 112-140.

(35) Cornell WD, Cieplak P, Bayly CI, Gould IR, Mez KM, Ferguson DM, Spellmeyer DC, Fox T, Caldwell JW, Kollman PA, *J. Am. Chem. Soc.* **1995**, *117*, 5179-5197

(36) Damm W, Frontera A, Tirado-Rives J, Jorgensen WL, *J. Comp. Chem.* **1997**, *18*, 1955-1970; Jorgensen WL, Maxwell DS, Tirado-Rives J, *J. Am. Chem. Soc.* **1996**, *118*, 11225-11236; JorgensenWL, Tirado-Rives J, *J. Am. Chem. Soc.* **1988**, *110*, 1657-1666; Kaminski G, Duffy EM, Matsui T, Jorgensen WL, *J. Phys. Chem.* **1994**, *98*, 13077-13082

(37) Jarzynski C, *Phys Rev Lett.* **1997**, *78*, 2690-2693

(38) Case DA, Darden TA, Cheatham ITE III, Simmerling CL, Wang J, Duke RE, Luo R, Walker RC, Zhang W, Mert KM, Roberts B, Hayik S, Roitberg A, Seabra G, Swails J, Götz AW, Kolossváry I, Wong KF, Paesani F, Vanicek J, Wolf RM, Liu J, Wu X, Brozell SR, Steinbrecher T, Gohlke H, Cai Q, Ye X, Wang J, Hsieh M-J, Cui G, Roe DR, Mathews DH, Seetin MG, Salomon-Ferrer R, Sagui C, Babin V, Luchko T, Gusarov S, Kovalenko A, Kollman PA (2012) AMBER 12. University of California, San Francisco

(39) Ewald P, *Ann. Phys.* **1921**, *64*, 253-287

(40) Frauenheim T, Porezag D, Elstner M, Jungnickel G, Elsner J, Haugk M, Sieck A, Seifert G, *Mat. Res. Soc. Symp. Proc.* **1998**, *491*, 91-104

(41) Elstner M, Porezag D, Jungnickel G, Elsner J, Haugk M, Frauenheim T, Suhai S, Seifert G, *Phys. Rev. B* **1998**, *58*, 7260-7268

(42) Seabra GM, Walker RC, Elstner M, Case DA, Roitberg AE, *J. Phys. Chem. A* **2007**, *111*, 5655-5664

(43) Walker RC, Crowley MF, Case DA, *J. Comp. Chem.* **2008**, *29*, 1019-1031